Microbial networks inferred from metabarcoding data lack replicability: consequences for next-generation biomonitoring

Charlie Pauvert[1], Jessica Vallance[2,3], Laurent Delière[2,4], Marc Buée[5], Corinne Vacher[1*]

[1]BIOGECO, INRA, Univ. Bordeaux, 33615 Pessac, France
[2]INRA, UMR 1065 Santé et Agroécologie du Vignoble, ISVV, F-33882 Villenave d'Ornon, France
[3]Université de Bordeaux, Bordeaux Sciences Agro, UMR 1065 SAVE, F-33175 Gradignan, France
[4]INRA, UE 1442 Vigne Bordeaux, F-33883 Villenave d'Ornon
[5]INRA, UMR 1136 Interactions Arbres/Micro-Organismes, F-54280, Champenoux, France

*** Correspondence**

Dr. Corinne Vacher

corinne.vacher@inra.fr

Keywords: Community ecology, Ecological networks, Species interaction networks, Microbiome, Pathobiome, Phyllosphere, DADA2, SparCC.

Abstract

Microbial interaction networks support many ecosystem services, including the regulation of crop diseases. One of the current challenges is automatically reconstructing these networks from metabarcoding data and monitoring their responses to environmental change. Here, we evaluated the ability of network inference methods to detect changes in crop-associated microbial networks. We used grapevine as a model plant system and assessed the impact of vineyard management (conventional *versus* organic) on the alpha- and beta-diversity of the fungal communities of grapevine leaves. We also inferred replicated networks of fungal associations, to compare network alpha- and beta-properties between management systems and to generate hypotheses concerning fungus-fungus interactions. We found that the richness, diversity and evenness of fungal communities were significantly higher in organic plots, and that community composition differed between management systems. *Erysiphe necator*, the causal agent of grapevine powdery mildew, was significantly more abundant in conventional plots, consistent with visual records of disease symptoms, whereas several yeast species were significantly more abundant in organic plots. Vineyard management also had a significant impact on the beta-properties of fungal association networks, but the high turnover of associations between plots precluded the generation of robust hypotheses concerning interactions between fungal taxa, casting doubts on the relationship between microbial association networks and plant health. Network inference methods therefore require improvement and validation before use in the next-generation biomonitoring of disease control services provided by the crop microbiota. As things stand, community-level data appear to be a more reliable and statistically powerful option than network-level data for monitoring the ecosystem services provided by the plant microbiota.

1 Introduction

Interactions between organisms and between organisms and their abiotic environment regulate the ecological processes underlying ecosystem services (Mace et al., 2012). Ecological interactions (e.g. predation, mutualism, parasitism) at a single point in space and time are usually represented as a network, with the organisms as nodes and the interactions as links (Pocock et al., 2012). Current challenges focus on understanding how and why these networks vary in space and time (Pilosof et al., 2017; Pellissier et al., 2018), and which network properties should be conserved or enhanced to sustain ecosystem services (Tylianakis et al., 2010; Montoya et al., 2012; Raimundo et al., 2018).

Global environmental changes due to human activities alter ecological networks by shifting species distributions and disrupting the interactions between species (Scheffers et al., 2016; Pecl et al., 2017). Agriculture, a key driver of global change (Tilman et al., 2002), has for instance an impact on both ecological communities (Tuck et al., 2014; Seufert and Ramankutty 2017) and ecological networks (Tylianakis et al., 2007; Macfadyen et al., 2009; Ma et al., 2019). Theoretical frameworks have been developed for the comparison of ecological networks between contrasting environmental conditions or along environmental gradients (Poisot et al., 2012; Tylianakis and Morris 2017; Pellissier et al., 2018; Delmas et al., 2019). By analogy with the α- and β-diversity of ecological communities, these frameworks define α- and β-properties for ecological networks, corresponding to whole-network metrics (e.g. connectance) and dissimilarities between pairs of networks, respectively (Pellissier et al., 2018).

Network ecology originates from the study of trophic links between macro-organisms (Ings et al., 2009) and initially ignored smaller organisms (Lafferty et al., 2006), but the importance of microorganisms is now recognized, with microbial interactions supplying ecosystem services such as biogeochemical cycling, provisioning services or disease regulation (Falkowski et al., 2008; van der Heijden et al., 2008; Berendsen et al., 2012). Microbial networks are affected by environmental changes (Creamer et al., 2016; Morriën et al., 2017), and it has been suggested that their properties could be used as potential bioindicators of environmental quality and ecosystem functioning (Karimi et al., 2017). The regulation of disease development in holobionts, defined as individual animals or plants together with all their associated microorganisms (Zilber-Rosenberg and Rosenberg 2008), is mediated by microbial interactions, including direct antagonistic interactions between the microbiota and pathogen species (Arnold et al., 2003; Koch and Schmid-Hempel, 2011; Kamada et al., 2013; Kemen 2014; Laur et al., 2018) and indirect interactions involving activation of the host immune system by the microbiota (Perazzolli et al., 2012; Kamada et al., 2013; Ritpitakphong et al., 2016; Vogel et al., 2016; Hacquard et al., 2017). The subset of a host-associated microbial network consisting of a pathogen and its interacting partners is known as the pathobiome (Vayssier-Taussat et al., 2014; Brader et al., 2017). The biomonitoring of holobiont health requires elucidation of the microbial interactions forming pathobiomes (Durán et al., 2018), identification of the network-level indicators of host disease susceptibility (Agler et al., 2016, Poudel et al., 2016) and monitoring of the impact of anthropogenic environmental change on these indicators. A combination of next-generation sequencing and machine-learning is required to achieve these objectives (Bohan et al., 2017; Derocles et al., 2018) and this study aimed to evaluate some of the methods developed to date.

Ecological networks have long been built on the basis of observations of ecological interactions. Meta-barcoding approaches are now providing additional information (Evans et al., 2016), and making it possible to generate hypotheses about interactions between organisms that are difficult to observe, such as microorganisms (Faust and Raes 2012; Berry and Widder 2014). Hypotheses concerning microbial interactions can be formulated on the basis of co-abundance data derived from environmental DNA

metabarcoding data (i.e. the sample × taxa matrix) via statistical or machine-learning approaches (Vacher et al., 2016). The representation of all positive and negative statistical associations between abundances for microbial taxa generally gives rise to a network resembling a hairball (Röttjers and Faust 2018). The challenge is to go beyond networks of this type, by removing spurious associations not due to microbial interactions and linking the remaining positive and negative associations to possible interaction mechanisms (Derocles et al., 2018). In a metabarcoding dataset, the total number of sequences per sample is arbitrary, imposed by the sequencer. Sequence counts contain only relative abundance information for species, and comparisons not taking this feature, known as compositionality, into account can result in the identification of artifactual associations (Gloor et al., 2017). Early methods of microbial network inference, such as SparCC (Friedman and Alm 2012), made use of log ratios of counts to overcome this bias. The second cause of spurious associations is the joint response of microbial taxa to abiotic or biotic factors, creating indirect associations reflecting taxon requirements, particularly for samples collected in heterogeneous environments (Röttjers and Faust 2018). Early studies dealt with this issue by first using regression to eliminate the environmental factors from the sequence counts and then inferring networks from the residuals (Jaskuschkin et al., 2016; Biswas et al., 2016). Several methods of network inference integrating environmental covariates, such as HMSC (Ovaskainen et al., 2017), PLN (Chiquet et al., 2018), FlashWeave (Tackmann et al., 2018) and MAGMA (Cougoul et al., 2018), have since been developed. Last, but not least, the taxonomic resolution of the nodes must be fine enough to capture variations in ecological interactions between microbial strains (Röttjers and Faust 2018). Novel bioinformatics approaches fully exploiting the resolution of molecular barcodes, such as DADA2 (Callahan et al., 2017), therefore seem highly appropriate. However, despite these advances, the inference of microbial networks from metabarcoding data is still in its infancy (Layeghifard et al., 2017), and inferred interactions should be interpreted with caution (Weiss et al., 2016; Röttjers and Faust 2018; Freilich et al., 2018; Barner et al., 2018; Zurell et al., 2018), because only a few validation experiments to date have been successful (Das et al., 2018; Wang et al., 2017).

In this study, we investigated whether changes in crop-associated microbial networks could be detected by combining current metabarcoding and network inference approaches. The monitoring of these changes is important, because these microbial networks possess intrinsic properties that hinder their invasion by pathogens (Murall et al., 2017) and form a barrier to disease development (Brader et al., 2017; Hacquard et al., 2017). Our objectives were (1) to assess the influence of crop management (conventional *versus* organic agriculture) on network α- and β-properties, (2) to investigate whether network-level properties are more sensitive to change than community-level properties and (3) to determine whether microbial networks can generate robust hypotheses concerning microbial interactions. We inferred microbial networks from multiple samples collected in homogeneous, replicated agricultural plots, using DADA2 (Callahan et al., 2016) and SparCC (Friedman and Alm 2012). We used grapevine as a model plant species and focused on the fungal component of its foliar microbiota, which contains several major pathogens.

2 Materials and methods

2.1 Study site and sampling design

Samples were collected in 2015, from an experimental vineyard (Fig. 1) located near Bordeaux (INRA, Villenave d'Ornon, France; 44°47'32.2"N 0°34'36.9"W). The experimental vineyard was planted in 2011 and was designed to compare three cropping systems: sustainable conventional agriculture (CONV), organic farming (ORGA) and pesticide-free farming (RESI) (Delière et al., 2014). The latter used a disease-resistant cultivar and was therefore not included in this study. The experiment had a randomized block design (Schielzeth and Nakagawa 2013) consisting of three blocks, each composed

of three plots, one for each of the cropping systems tested. Each plot covered an area of 2100 m^2 and was composed of 20 rows of 68 vines each, with a 1.60 m between rows and 0.95 m between vines in a single row.

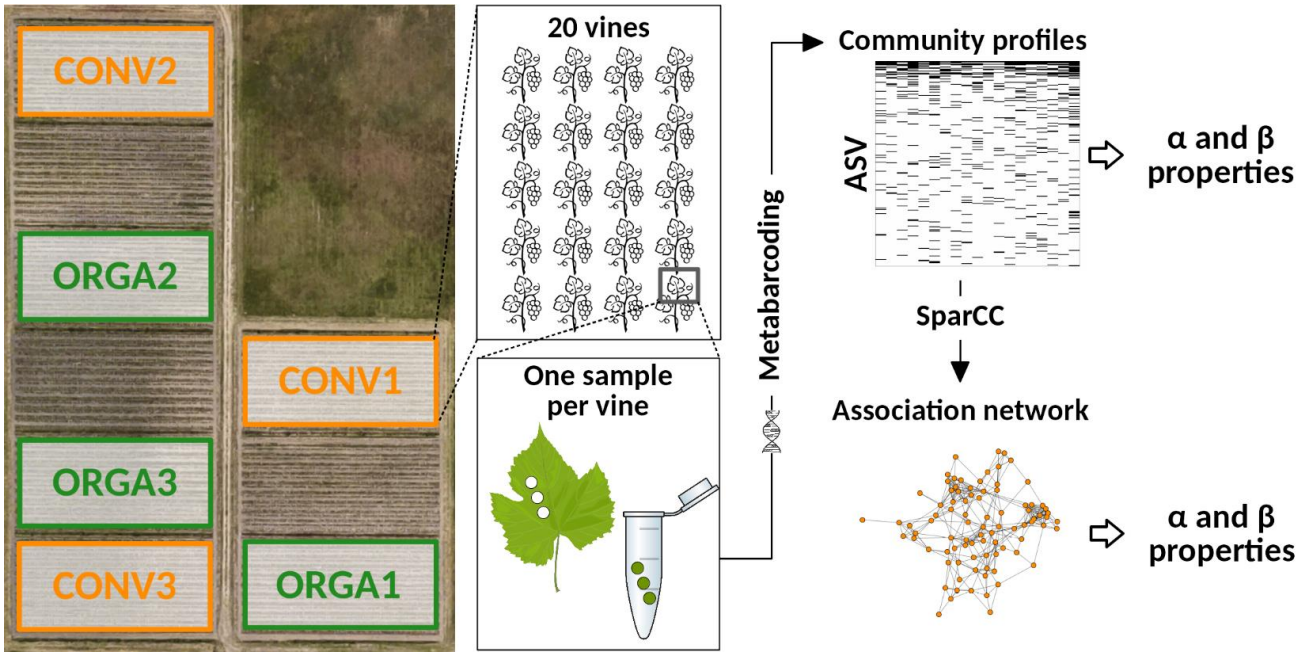

Figure 1 – **Experimental design**. Foliar fungal communities were characterized in three conventional (CONV) and three organic (ORGA) vineyard plots by a metabarcoding approach. We analyzed 20 foliar samples per plot. For each plot, we thus obtained 20 community profiles (described in terms of amplicon sequence variants (ASV)) and one association network (inferred with the SparCC software developed by Friedman et al., 2012). More networks were then obtained by varying network reconstruction parameters (Fig. 5). The effects of cropping system (CONV versus ORGA) on the grapevine foliar microbiota were assessed with both community and network α- and β-properties.

The same cultivar – *Vitis vinifera* L. cv. Merlot noir grafted onto a 3309 C rootstock – was used in both the CONV and ORGA cropping systems. CONV plots were managed according to the general principles of integrated pest management (IPM), as listed in Appendix III of the 2009/128/EC Directive (European Commission 2009). ORGA plots were managed according to European Council Regulation (EC) No 834/2007 (European Commission 2007). ORGA plots were treated with copper and sulfur-based products, whereas additional phytosanitary products were allowed in CONV plots (Table S1). The cropping systems differed in terms of the types of pesticides applied and the timing of applications, but not in terms of doses (Table S1). All products and active ingredients were applied between the end of April and mid-August of 2015. Grapes were harvested on September 10, 2015. The incidence and severity of disease at harvest were higher in CONV plots than in ORGA plots for both powdery mildew (caused by the fungal pathogen *Erysiphe necator*) and black rot (caused by the fungal pathogen *Guignardia bidwellii*). Downy mildew symptoms (caused by the oomycete pathogen *Plasmopara viticola*) did not differ significantly between cropping systems (Table S2).

Grapevine leaves were collected a couple hours before grape harvest, from 20 vines per plot in the CONV and ORGA plots. Edge effects were avoided by selecting the 20 vines from the center of each plot. The third leaf above the grapes was collected from each vine, placed in an individual bag and immediately transported to the laboratory. In total, 120 leaves, corresponding to 1 leaf × 20 vines × 3 plots × 2 cropping systems, were therefore collected. Leaves were processed on the day of collection,

with sterilized tools in the sterile field of a MICROBIO electric burner (MSEI, France). Three contiguous discs, each 6 mm in diameter, were cut from the center of each leaf, approximately 2 cm from the midrib. They were placed in the well of a sterile DNA extraction plate. The leaf disks were then freeze-dried overnight (Alpha 1-4 DA Plus, Bioblock Scientific).

2.2 DNA extraction and sequencing

Leaf disks (Fig. 1) were ground with a single-glass ball mill (TissueLyser II, Qiagen) and DNA was then extracted with a CTAB chloroform/isoamyl alcohol (24:1) protocol. A dozen "empty" wells (*i.e.* containing nothing but extraction reagents) were included on each plate as negative control samples for DNA extraction. Three of these negative control samples were randomly selected and pooled before sequencing. Three replicates of a fungal mock community, each consisting of an equimolar pool of DNA from 189 pure fungal strains, were also included as positive control samples (Pauvert et al., 2019).

The nuclear ribosomal internal transcribed spacer (ITS) region, which is considered to be the universal barcode region for fungi (Schoch et al., 2012), was then amplified with the ITS1F (5'-CTTGGTCATTTAGAGGAAGTAA-3', Gardes and Bruns 1993) and ITS2 (5'-GCTGCGTTCTTCATCGATGC-3', White et al., 1990) primer pair, which targets the ITS1 region. PCR was performed in an Eppendorf thermocycler (Eppendorf), with a reaction mixture (25 µl final volume) consisting of 0.04 U *Taq* polymerase (SilverStar DNA polymerase, Eurogentec), 1X buffer, 2 mM $MgCl_2$, 200 µM of each dNTP, 0.2 µM of each primer, 1 $ng.\mu l^{-1}$ bovine serum albumin (New England BioLabs) and 2 µl DNA template. A pseudo-nested PCR protocol was used, with the following cycling parameters: enzyme activation at 95°C for 2 min; 20 (1^{st} PCR with regular primers; Table S3) and then 15 (2^{nd} nested PCR with pre-tagged primers; Table S3) cycles of denaturation at 95°C for 30 s, 53°C for 30 s, 72°C for 45 s; and a final extension phase at 72°C for 10 min. "Empty" wells (i.e. containing nothing but PCR reagents) were included on each plate as a negative control for PCR. Three negative control samples were randomly selected and pooled before sequencing. In addition, the six PCR products corresponding to the 24^{th} leaf of the six plots under study (three CONV plots, three ORGA plots) were split in two, with each half of the sample sequenced independently to serve as technical replicates for sequencing.

We checked the quality of all the PCR products by electrophoresis in 2% agarose gels. PCR products were purified (CleanPCR, MokaScience), multiplex identifiers and sequencing adapters were added, and library sequencing on an Illumina MiSeq platform (v3 chemistry, 2×250 bp) and sequence demultiplexing (with exact index search) were performed at the Get-PlaGe sequencing facility (Toulouse, France).

2.3 Bioinformatic analysis

Based on the mock community included in the sequencing run, we found that analyzing single forward (R1) sequences with DADA2 (Callahan et al., 2016) was a good option for fungal community characterization (Pauvert et al., 2019). Using DADA2 v1.6, we retained only R1 reads with less than one expected error (based on quality scores; Edgar and Flyvbjerg, 2015) that were longer than 100 bp, and we then inferred amplicon sequence variants (ASV) for each sample. Chimeric sequences were identified by the consensus method of the *removeBimeras* function. Taxonomic assignments were performed with RDP classifier (Wang et al., 2007), implemented in DADA2 and trained with the UNITE database v. 7.2 (UNITE Community 2017). Only ASVs assigned to a fungal phylum were retained. The ASV table was then filtered as described by Galan et al., (2016) with a homemade script (https://gist.github.com/cpauvert/1ba6a97b01ea6cde4398a8d531fa62f9). The script removed ASVs from all samples for which the number of sequences was below the cross-contamination threshold,

defined as their maximum number in negative control samples (Galan et al., 2016). Finally, we checked the compositional similarity of the technical replicates (Fig. S1), retaining the sample with the largest number of sequences for each replicate. The final ASV table contained 1116 ASVs, 112 samples and 4,760,068 high-quality sequences (Table S4).

2.4 Statistical analyses

Statistical analyses were performed with R software v3.4.1 (R Core Team 2017), with the packages lme4 (Bates et al., 2015), vegan (Oksanen et al., 2018), permute (Simpson 2016), phyloseq (McMurdie and Holmes 2013) including the DESeq2 extension (Love et al., 2014), and igraph (Csardi and Nepusz 2006). Data were manipulated and plots were created with reshape2, plyr and ggplot2 (Wickham 2007; 2011; 2016), cowplot (Wilke 2018), ggraph (Pedersen 2018) and VennDiagram (Chen 2018).

2.4.1 Effect of cropping system on community α-diversity

Generalized linear mixed models (GLMMs) were used to test the effect of cropping system on the richness, diversity and evenness of fungal communities. The models included the cropping system as a fixed treatment effect, the block and its interaction with the cropping system as random factors, and the sampling depth (defined as the total number of raw sequences per sample) as an offset (Bálint et al., 2015; McMurdie and Holmes 2014). Community richness was defined as the number of ASVs per sample. We used a logarithmic link function to model these count data, assuming a negative binomial distribution to deal with overdispersion (Zuur et al., 2009). Community diversity was measured with the Inverse Simpson index (Simpson 1949) and modeled with a Gaussian distribution and the logarithmic link function. Evenness was estimated with Pielou's index (Pielou 1966) and modeled with a Gaussian distribution and the logarithmic link function. The offset was transformed according to the link function. The significance of the fixed treatment effect was finally assessed with the Wald χ^2 test (Bolker et al., 2009).

2.4.2 Effect of cropping system on community β-diversity

Permutational analyses of variance (PERMANOVAs; Anderson 2001) were used to evaluate the effect of cropping system on compositional dissimilarities between fungal communities detected with the quantitative and binary versions of the Jaccard dissimilarity index (Chao et al., 2006; Jaccard 1900). The models included cropping system, sampling depth (log-transformed) and their interaction as fixed effects. Permutations (n = 999) were constrained within blocks. ASVs differing in abundance between cropping systems were identified with DESeq2 (Love et al., 2014), by calculating the likelihood ratio between a full model including block and cropping system as fixed effects and a simplified model including only the block factor. The estimated fold-changes in abundance were considered significant if the p-value was below 0.05 after Benjamini and Hochberg adjustment.

2.4.3 Effect of cropping system on network α-properties

Fungal association networks were inferred at plot level (Fig. 1) with the SparCC algorithm (Friedman and Alm 2012) implemented in FastSpar (Watts et al., 2019) with default SparCC values. Ten networks per plot were constructed by varying the percentage P of ASVs included in the network (with P ranging from 10% to 100% of the most abundant ASVs in the plot). Networks had ASVs as nodes and a positive or negative link between ASVs in cases of significant associations between abundance. Six α-properties were calculated for all networks: number of links, network density, number of connected components, diameter of the largest component, mean node degree and proportion of negative links (Table S5). The effect of cropping system on these properties was investigated by performing Wilcoxon rank-sum tests for every value of P. The Benjamini-Hochberg procedure was used to correct p-values for multiple testing.

2.4.4 Effect of cropping system on network β-properties

The topological distance between networks was calculated for all pairs of networks, with the *D* index defined by Schieber et al., (2017) for binary networks. The dissimilarity of associations between networks, β_{WN} according to the framework described by Poisot et al., (2012), was then calculated for all pairs of networks with the binary Jaccard dissimilarity index. β_{WN} was then partitioned into two components (Poisot et al., 2012): the dissimilarity of associations between ASVs common to both networks (β_{OS}) and the dissimilarity of associations due to species turnover (β_{ST}). PERMANOVA was used to evaluate the effect of cropping system on the topological distance between networks (*D*) and the dissimilarity of associations between networks (β_{WN}, β_{ST} and β_{OS}). The models included cropping system, *P* and their interactions as fixed effects. The permutations (*n*=999) were constrained within blocks. Consensus networks were built to identify robust associations that could indicate biotic interactions between fungal strains.

3 Results

The foliar fungal communities were dominated by Ascomycota in both ORGA (87.2% of sequences) and CONV (96.8%) plots. They were largely colonized by an ASV assigned to the *Aureobasidium* genus. More than half the sequences belonged to this ASV (Table 1), whatever the cropping system. The causal agent of powdery mildew, *Erysiphe necator*, was among the 10 most abundant fungal species. The proportion of sequences assigned to this pathogen species was higher in CONV than in ORGA plots (Table 1), consistent with the visual records of disease symptoms (Table S2).

ASV taxonomic assignment	**TOTAL**		**ORGA**		**CONV**	
	Rank	RA	Rank	RA	Rank	RA
Aureobasidium sp.	1	61.4	1	55.8	1	66.7
Cladosporium delicatulum	2	6.3	4	6.9	2	5.8
Filobasidium sp.	3	5.1	2	9.7	9	0.7
Alternaria sp.	4	4.4	5	3.9	4	5.0
Epicoccum nigrum	5	4.1	7	2.7	3	5.4
Cladosporium ramotenellum	6	3.5	3	7	46	<0.1
Mycosphaerella tassiana	7	3.3	8	1.8	5	4.8
Didymella sp.	8	1.4	6	2.7	33	0.1
Erysiphe necator	9	1.1	38	<0.1	6	2
Vishniacozyma victoriae	10	0.9	9	1.6	17	0.3

Table 1 - Most abundant amplicon sequence variants (ASVs) in grapevine foliar fungal communities according to cropping system. The relative abundances (RA, in %) and ranks of ASVs were calculated for all leaf samples (TOTAL; *n* = 112) and for samples collected from organic (ORGA; *n* = 55) and conventional plots (CONV; *n* = 57).

3.1 Effect of cropping system on community α- and β-diversity

Fungal community richness, diversity and evenness were significantly higher in ORGA than CONV plots (Wald $\chi^2 = 4.74$, $p = 0.029$; Wald $\chi^2 = 8.28$, $p = 0.004$; Wald $\chi^2 = 12.88$, $p < 0.001$, respectively; Fig. 2). The composition of foliar fungal communities differed significantly between cropping systems (Table 2), in terms of both the relative abundance (Fig. 3A) and presence-absence of ASVs (Fig. 3B). DESeq2 analysis revealed that four ASVs, including the fungal pathogen *Erysiphe necator*, were significantly more abundant in CONV plots, whereas 10 other ASVs, including several yeast species (from the genera *Vishniacozyma*, *Sporobolomyces* and *Filobasidium*), were significantly more abundant in ORGA plots (Fig. 3C). Principal coordinate analysis (PCoA) with the Jaccard quantitative index (Fig. 3A) revealed large differences in the relative abundances of ASVs between samples within a cropping system. The first axis of the PCoA accounted for 32.5% of the variance in community composition but did not discriminate between cropping systems. It was significantly correlated with the relative abundance of the dominant ASV (assigned to the *Aureobasidium* genus) (Spearman $\rho = 0.96$; $p < 0.001$).

Dissimilarity index	**PERMANOVA**				
Quantitative Jaccard	**Variable**	**Df**	***F***	**R2**	**Pr(>F)**
	Sequencing_Depth (SD)	1	4.49	0.04	**<0.01**
	Cropping_System (CS)	1	9.42	0.08	**<0.01**
	SD × CS	1	1.17	0.01	0.26
	Residuals	108		0.854	
	Total	111		1	
Binary Jaccard	**Variable**	**Df**	***F***	**R2**	**Pr(>F)**
	Sequencing_Depth (SD)	1	1.05	0.01	0.29
	Cropping_System (CS)	1	5.21	0.05	**<0.01**
	SD × CS	1	1.03	0.01	0.41
	Residuals	108		0.937	
	Total	111		1	

Table 2 – Effect of cropping system — conventional *versus* organic — on the β-diversity metrics of grapevine foliar fungal communities. Dissimilarities in community composition between samples were assessed with both the quantitative and binary Jaccard indices. The effects of sequencing depth (SD, log-transformed) and cropping system on composition dissimilarities between communities were evaluated in permutational analyses of variance (PERMANOVA). The number of permutations was set to 999 and permutations were constrained by block.

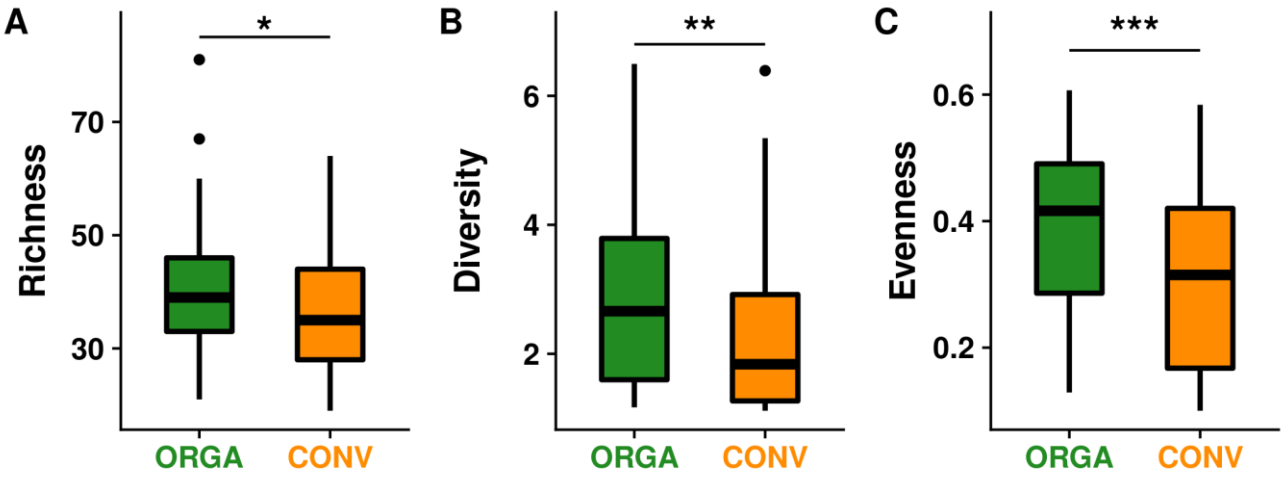

Figure 2 - Effect of cropping system —conventional (CONV) versus organic (ORGA) — on the α-diversity metrics of grapevine foliar fungal communities. (A) Community richness, defined as the number of ASVs. (B) Community diversity, measured with the inverse Simpson index. (C) Community evenness, measured with Pielou's index. Differences in α-diversity metrics between cropping systems were evaluated in Wald χ^2 tests (* p<0.05; **p<0.01; ***p<0.001).

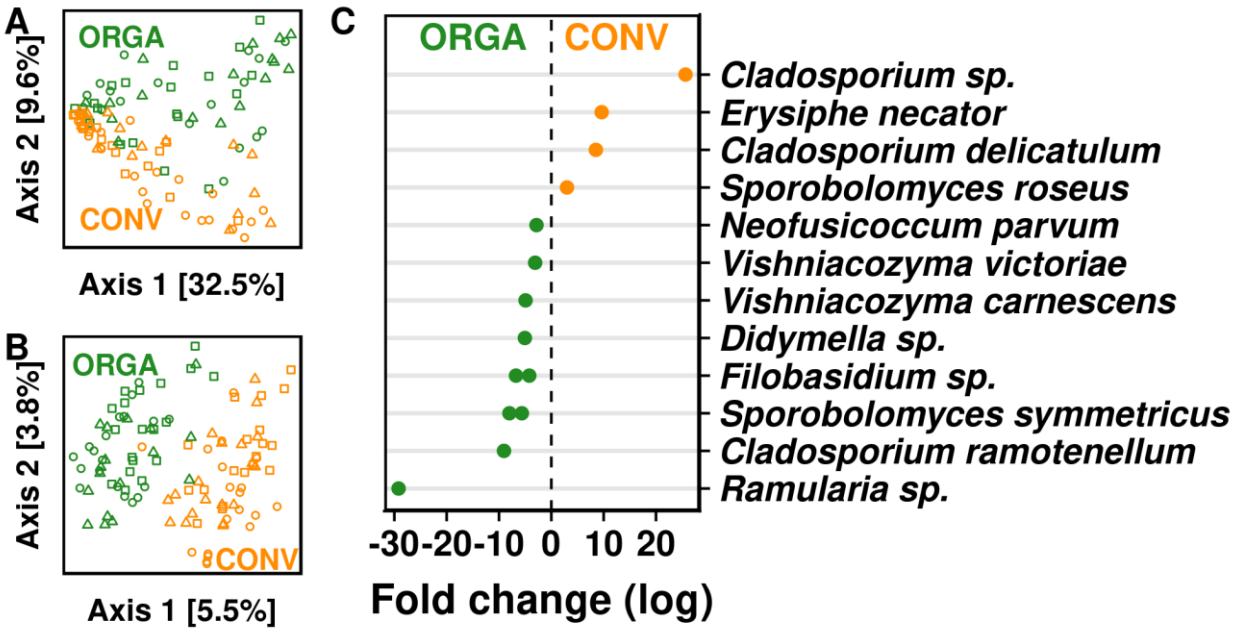

Figure 3 - Effect of cropping system — conventional (CONV) versus organic (ORGA) — on the β-diversity metrics of grapevine foliar fungal communities. Principal coordinate analyses (PCoA) were used to represent dissimilarities in composition between samples, as assessed with the (A) quantitative and (B) binary Jaccard indices. The effect of cropping system on both β-diversity metrics was significant (Table 2). Green circles, squares and triangles correspond to samples collected in the ORGA1, ORGA2 and ORGA3 plots, respectively. Orange circles, squares and triangles correspond to the CONV1, CONV2 and CONV3 plots, respectively (Fig. 1). (C) Log-transformed ratio of ASV relative abundance in CONV plots over that in ORGA plots, for 14 ASVs identified as differentially abundant between cropping systems by DESeq2 analysis followed by Benjamini-Hochberg adjustment (Love et al., 2014).

3.2 Effect of cropping system on network α- and β-properties

In total, we obtained 60 fungal association networks, corresponding to six plots (Fig. 1) per *P* category (Fig. 4A). None of the six network α-properties (Table S5) differed between cropping systems (Table S6), but all were significantly correlated with the percentage *P* of ASVs included in the network (Table S7). The total number of links and the mean degree increased with *P*, whereas the number of connected components, network diameter, connectance and the proportion of negative links decreased (Fig. 4B; Table S7). Similarly, the topological distance between networks did not differ between cropping systems, but was influenced by *P* (Table 3). By contrast, cropping system had a significant effect on the overall dissimilarity of associations (β_{WN}) and the dissimilarity of associations between shared ASVs (β_{OS}; Table 3 and Fig. 5). Fungal associations also varied considerably between plots within a cropping system (Fig. 4A and Fig. 6). When all ASVs were used for network construction (*P*=100%), only two associations were common to all three network replicates of the ORGA system (Fig. 6A; Fig. S2A) and only six were common to all three network replicates of the CONV system (Fig. 6B; Fig. S2B). The two associations replicated in the ORGA system were negative associations between the dominant ASV (assigned to the genus *Aureobasidium*) and *Cladosporium ramotenellum*, and between *Vishniacosyma victoriae* and *Neofusicoccum parvum* (Fig. S2A). Five of the six associations replicated in the CONV system were positive, the remaining negative association being that between the dominant ASV (assigned to the genus *Aureobasidium*) and *Epicoccum nigrum* (Fig. S2B). No association common to all six networks was identified (Fig. 6C).

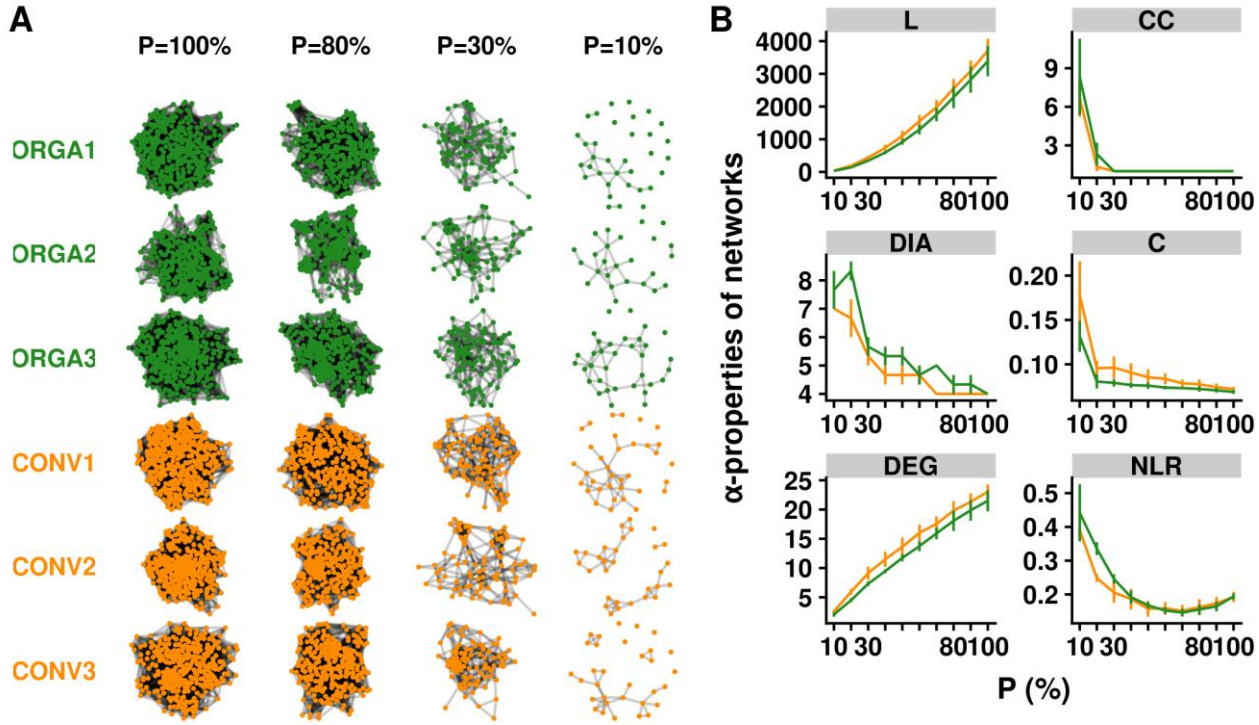

Figure 4 - Effect of cropping system — conventional (CONV) *versus* organic (ORGA) — on the α-properties of grapevine foliar fungal networks. (A) Association networks inferred from fungal metabarcoding data with SparCC (Friedman and Alm 2012). A total of 60 networks were inferred, corresponding to 2 cropping systems × 3 replicates (blocks) × 10 *P* values, with *P* the percentage of most abundant ASVs used for network inference. Only four values of *P* are shown on the figure. (B) Variations in network α-properties**.** The following properties (Table S5) were calculated for each network: the number of links (L) and connected components (CC), the network diameter (DIA) and connectance (C) and the mean degree (DEG) and negative link ratio (NLR). The percentage *P* of ASVs used for network reconstruction had a significant influence on all properties (Table S7), whereas cropping system did not (Table S6).

Dissimilarity index	**PERMANOVA**				
Topological dissimilarity (Schieber's D)	**Variable**	**Df**	***F***	**R2**	**Pr(>F)**
	Percent_ASV (P)	1	57.75	0.50	**<0.01**
	Cropping_System (CS)	1	1.72	0.01	0.19
	P × CS	1	0.65	0.01	0.51
	Residuals	56		0.48	
	Total	59		1	
Overall dissimilarity of associations (β_{WN})	**Variable**	**Df**	***F***	**R2**	**Pr(>F)**
	Percent_ASV (P)	1	2.41	0.04	**<0.01**
	Cropping_System (CS)	1	5.0	0.08	**<0.01**
	P × CS	1	2.21	0.03	**<0.01**
	Residuals	56		0.85	
	Total	59		1	
Dissimilarity of associations between shared ASVs (β_{OS})	**Variable**	**Df**	***F***	**R2**	**Pr(>F)**
	Percent_ASV (P)	1	0.53	0.01	0.61
	Cropping_System (CS)	1	11.07	0.16	**<0.01**
	P × CS	1	0.56	0.01	0.57
	Residuals	56		0.798	
	Total	59		1	
Dissimilarity of associations due to ASV turnover (β_{ST})	**Variable**	**Df**	***F***	**R2**	**Pr(>F)**
	Percent_ASV (P)	1	1.30	0.02	**<0.01**
	Cropping_System (CS)	1	0.27	<0.01	1.00
	P × CS	1	1.30	0.02	**<0.01**
	Residuals	56		0.95	
	Total	59		1	

Table 3 – Effect of cropping system — conventional *versus* organic — on the β-properties of grapevine foliar fungal networks. The D index quantifies the topological dissimilarity between networks (Schieber et al., 2017) whereas the other three metrics (β_{WN}, β_{OS} and β_{ST}), which were calculated with the binary Jaccard index, quantify differences in associations between networks (Poisot et al., 2012). The effect of the percentage *P* of the most abundant ASVs used for network inference, and the effect of cropping system on the dissimilarities between networks were evaluated in permutational analyses of variance (PERMANOVA). The number of permutations was set to 999 and permutations were constrained by block.

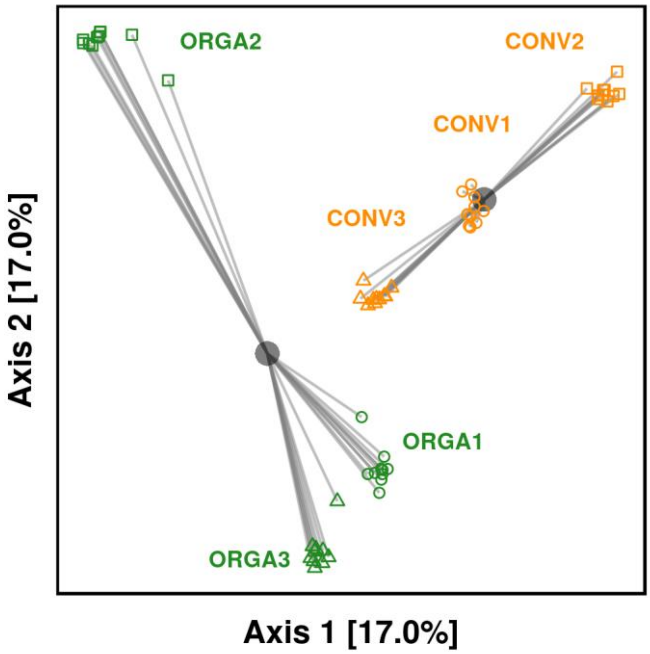

Figure 5 - Effect of cropping system —conventional (CONV) *versus* organic (ORGA) — on the β-properties of grapevine foliar fungal networks. Principal coordinate analysis (PCoA) representing dissimilarities between networks, measured with the β_{OS} index (Poisot et al., 2012) calculated with the binary Jaccard index. β_{OS} measures the dissimilarity between two networks in terms of the presence-absence of associations between shared ASVs. The centroids for each cropping system are represented by gray circles. The effect of cropping system on β_{OS} was significant (Table 3).

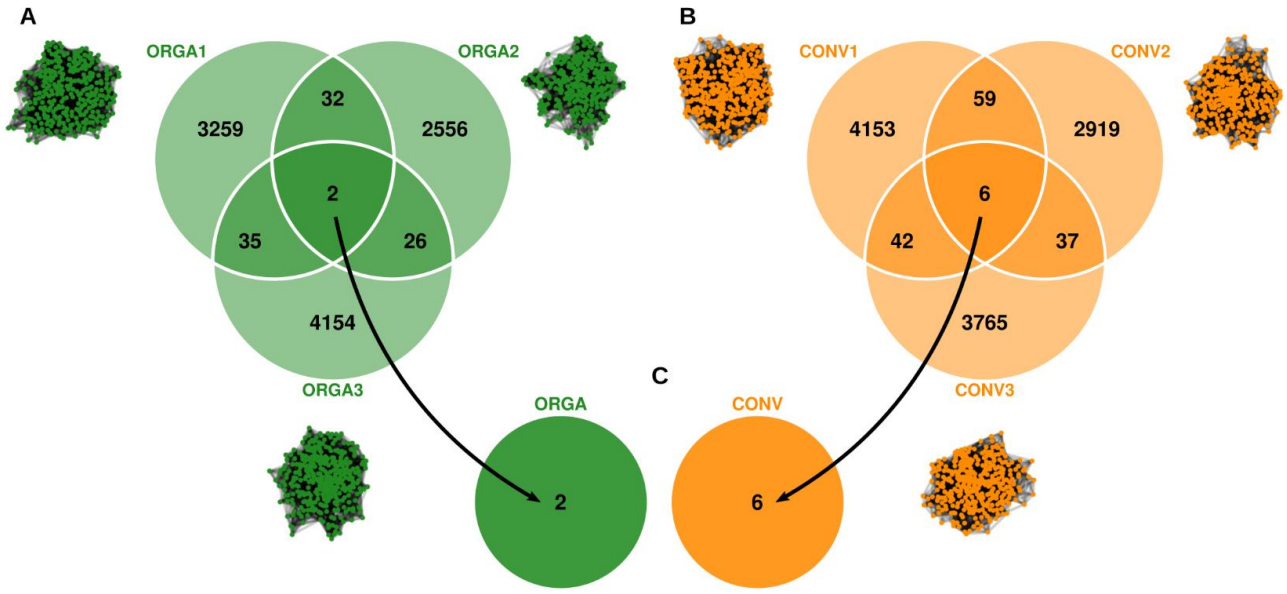

Figure 6 - Venn diagrams showing the number of fungal associations common to network replicates. (A) Associations common to the three network replicates inferred for the organic cropping system (ORGA1, ORGA2, ORGA3) and (B) the three network replicates inferred for the conventional cropping system (CONV1, CONV2, CONV3), regardless of the sign of the association, in the situation in which all ASVs were used for network construction (*P*=100%). (C) Associations common to the six networks.

4 Discussion

Plant-associated microbial interaction networks protect plants against disease (Kemen 2014; Hassani et al., 2018). There is, therefore, a crucial need to monitor their responses to drivers of environmental change, such as agricultural practices. Here, we assessed the effects of cropping system (organic *versus* conventional) on plant-associated microbial communities and networks, using grapevine as a model plant. We focused on the fungal component of the grapevine foliar microbiota because it contains several pathogen species. We analyzed both microbial community α- and β-diversities and microbial network α- and β-properties, to determine whether network-level metrics were better indicators of environmental change than community-level metrics (Karimi et al., 2017, Ma et al., 2018). We found that the α-properties of microbial networks (i.e. whole-network metrics; Pellissier et al., 2018) did not differ between cropping systems. Their variations were correlated with the percentages of the most abundant taxa included in the network, which is a network inference methodological parameter. By contrast, some β-properties of microbial networks differed significantly between cropping systems, revealing a difference in microbial associations between organic and conventional vineyards. This difference remained significant when network pairwise comparisons were based on shared taxa only, suggesting that the differences between organic and conventional networks were due to re-associations of fungal taxa rather than a turnover of taxa. As expected from previous results, microbial community α- and β-diversities differed significantly between cropping systems. Our results therefore indicate that both community-level and network-level metrics can be used to monitor changes in the crop microbiota. Using our findings, we tried to determine which metrics were most likely to contain information about plant health.

Community-level analyses showed that the richness, diversity and evenness of the grapevine foliar microbiota were significantly higher in organic than conventional vineyards, consistent with the recent findings of Kernaghan et al. (2017) (but see Castañeda et al., 2018). The cropping system also significantly affected the composition of grapevine foliar fungal communities, as reported in previous studies (Schmid et al., 2011; Pancher et al., 2012; Varanda et al., 2016; Kernaghan et al., 2017; Castañeda et al.,, 2018). Several fungal taxa differed significantly in abundance between cropping systems. For instance, *Erysiphe necator,* the causal agent of grapevine powdery mildew, was significantly more abundant in conventional than in organic plots. These results are consistent with visual assessments of disease symptoms, indicating that, despite their numerous biases, metabarcoding data do contain some quantitative information useful for monitoring plant disease development (Sapkota et al., 2015; Jakuschkin et al., 2016; Makiola et al., 2018). Several yeast strains, assigned to the genera *Vishniacozyma*, *Sporobolomyces* and *Filobasidium*, were significantly more abundant in organic plots. These yeast genera are frequently detected on leaf surfaces due to their tolerance of irradiation and they might influence plant growth by producing plant hormone-like metabolites (Kemler et al., 2017).

Network-level comparisons revealed an unexpectedly high degree of variability between network replicates within each cropping system. Replicate microbial networks for the same cropping system had very few associations in common, and no association was consistent found to be common to both cropping systems. Only two associations were common to all three replicates of the organic system. Both were negative and involved two plant pathogens — *Neofusicoccum parvum* (Bruez et al., 2014) and *Cladosporium ramotenellum* (Swett et al., 2016) — and two other species known to have antagonistic effects on plant pathogens: *Vishniacozyma victoriae* and *Aureobasidium sp* (Pertot et al., 2017; Gramisci et al., 2018). These hypothetical fungus-fungus interactions appear to be relevant but require experimental validation, to demonstrate that networks do contain information about plant health-related mechanisms. Several methodological biases might account for the high variability of

fungal associations within a cropping system (i.e. the low replicability of microbial association networks). First, each network was built from 20 samples, whereas a minimum of 25 samples is generally recommended to obtain reliable networks (Berry and Widder 2014). Second, network nodes (i.e. amplicon sequence variants) may group together fungal strains with different interaction traits (McLaren and Callahan, 2018), despite their fine-scale taxonomic resolution (Callahan et al., 2017). Third, microbial associations may be triggered by spatial variations in environmental conditions (i.e. microclimate or leaf traits) rather than by biotic interactions (Derocles et al., 2018; Freilich et al., 2018). However, this third hypothesis is not particularly likely in our experimental system because the vineyard plots were adjacent to each other and planted with grapevine clones. The sampling design also limited microclimate variations, because we collected all leaves in less than two hours and controlled for the position of the sampled leaf on the vine. Alternatively, the associations detected may reflect the real interactions between fungal taxa. The turnover of associations might, in that case, be due to the functional redundancy of fungal taxa. Taxonomically different communities, involving different interactions between members, may have similar functions (Louca et al., 2016) and protect plant health in a similar way.

Based on these findings, we cannot recommend the use of network properties for monitoring the disease regulation services provided by the microbiota. The replicated microbial association networks inferred from metabarcoding data were highly variable within each set of environmental conditions and generated few robust hypotheses concerning interactions between fungi, precluding their use to monitor the barrier effect of microbial interactions against pathogens. By contrast, community-level metrics revealed clear-cut changes in the plant microbiota in response to environmental change and reflected the disease status of the plant. Moreover, they were more statistically powerful than network-level metrics, because many samples were required to infer each microbial network replicate. Hence, as things stand, machine-learning approaches using community-level microbial metabarcoding data (Cordier et al., 2018) appear to be a more reliable option for the next-generation biomonitoring of ecosystem services than microbial network inference.

5 Conflict of Interest

The authors declare that there is no conflict of interest.

6 Authors' Contributions

CP performed the bioinformatic and statistical analyses and wrote the first draft of the manuscript. JV and CV performed the sampling and processed the leaf samples. LD managed the sampling site and provided data on phytosanitary treatments and disease symptoms. JV performed the DNA extractions and amplifications. MB coordinated the creation of the fungal mock community and the sequencing of all samples. CV conceived the study, supervised the analyses and made a major contribution to the writing of the final draft. All authors discussed the preliminary version of the results and revised the manuscript.

7 Funding

We thank the INRA MEM metaprogram (Meta-Omics of Microbial Ecosystems) for financial and scientific support. Sequencing was funded by the INRA MEM MetaBAR project and bioinformatic and statistical analyses were performed as part of the INRA MEM Learn-biocontrol project. Additional funding was received from the LABEX COTE (ANR-10-LABX-45), the LABEX CEBA (ANR-10-LABX-25-01) and INRA EcoServ metaprogram on ecosystem services (IBISC project) and the Aquitaine Region (Athene project, n°2016-1R20301-00007218). CP's PhD grant was funded by the

INRA and Bordeaux Sciences Agro (BSA). The management of the experimental site was partly funded by the AFB (French Agency for Biodiversity) within the DEPHY network.

8 Acknowledgments

We thank Dave Bohan, Lucile Muneret, Andreas Makiola and all members of the ANR NGB Consortium (ANR-17-CE32-0011) for helpful scientific exchanges on next-generation biomonitoring and for their comments on the manuscript. We also thank Gregory Gambetta, Guilherme Martins, Frédéric Barraquand, Isabelle Lesur and Adrien Rush for useful comments on preliminary results. We thank the Genotoul sequencing facility (Get-PlaGe) for sequencing and the Genotoul bioinformatics facility (Bioinfo Genotoul) for providing computing and storage resources. We also thank Julie Sappa from Alex Edelman & Associates for English language revision.

9 Data availability

The raw sequence data were deposited in Dataverse and are available in the FASTQ format at https://doi.org/10.15454/3DPFN. The code is available as an archive at https://doi.org/10.15454/NSHUAQ.

REFERENCES

Agler, M. T., Ruhe, J., Kroll, S., Morhenn, C., Kim, S.-T., Weigel, D., et al. (2016). Microbial hub taxa link host and abiotic factors to plant microbiome variation. *PLoS Biology* 14, e1002352. doi:10.1371/journal.pbio.1002352.

Anderson, M. J. (2001). A new method for non- parametric multivariate analysis of variance. *Austral Ecology* 26, 32–46. doi:10.1111/j.1442-9993.2001.01070.pp.x.

Arnold, A. E., Mejía, L. C., Kyllo, D., Rojas, E. I., Maynard, Z., Robbins, N., et al. (2003). Fungal endophytes limit pathogen damage in a tropical tree. *PNAS* 100, 15649–15654. doi:10.1073/pnas.2533483100.

Bálint, M., Bartha, L., O'Hara, R. B., Olson, M. S., Otte, J., Pfenninger, M., et al. (2015). Relocation, high- latitude warming and host genetic identity shape the foliar fungal microbiome of poplars. *Molecular Ecology* 24, 235–248. doi:10.1111/mec.13018.

Barner, A. K., Coblentz, K. E., Hacker, S. D., and Menge, B. A. (2018). Fundamental contradictions among observational and experimental estimates of non- trophic species interactions. *Ecology* 99, 557–566. doi:10.1002/ecy.2133.

Bates, D., Mächler, M., Bolker, B., and Walker, S. (2015). Fitting linear mixed-effects models using lme4. *Journal of Statistical Software* 67, 1–48. doi:10.18637/jss.v067.i01.

Berendsen, R. L., Pieterse, C. M. J., and Bakker, P. A. H. M. (2012). The rhizosphere microbiome and plant health. *Trends Plant Sci.* 17, 478–486. doi:10.1016/j.tplants.2012.04.001.

Berry, D., and Widder, S. (2014). Deciphering microbial interactions and detecting keystone species with co-occurrence networks. *Frontiers in Microbiology* 5, 219. doi:10.3389/fmicb.2014.00219.

Biswas, S., Mcdonald, M., Lundberg, D. S., Dangl, J. L., and Jojic, V. (2016). Learning microbial interaction networks from metagenomic count data. *Journal of Computational Biology : a journal of computational molecular cell biologyy.* 23, 526–535. doi:10.1089/cmb.2016.0061.

Bohan, D. A., Vacher, C., Tamaddoni-Nezhad, A., Raybould, A., Dumbrell, A. J., and Woodward, G. (2017). Next-Generation Global Biomonitoring: Large-scale, Automated Reconstruction of Ecological Networks. *Trends in Ecology & Evolution* 32, 477–487. doi:10.1016/j.tree.2017.03.001.

Bolker, B. M., Brooks, M. E., Clark, C. J., Geange, S. W., Poulsen, J. R., Stevens, M. H. H., et al. (2009). Generalized linear mixed models: a practical guide for ecology and evolution. *Trends Ecol. Evol. (Amst.)* 24, 127–135. doi:10.1016/j.tree.2008.10.008.

Brader, G., Compant, S., Vescio, K., Mitter, B., Trognitz, F., Ma, L.-J., et al. (2017). Ecology and genomic insights on plant-pathogenic and -nonpathogenic endophytes. *Annual Review of Phytopathology* 55, 61–83. doi:10.1146/annurev-phyto-080516-035641.

Bruez, E., Vallance, J., Gerbore, J., Lecomte, P., Costa, J.-P. D., Guerin-Dubrana, L., et al. (2014). Analyses of the temporal dynamics of fungal communities colonizing the healthy wood tissues

of esca leaf-symptomatic and asymptomatic vines. *PLoS ONE* 9, e95928. doi:10.1371/journal.pone.0095928.

Callahan, B. J., McMurdie, P. J., and Holmes, S. P. (2017). Exact sequence variants should replace operational taxonomic units in marker-gene data analysis. *The ISME Journal* 11, 2639–2643. doi:10.1038/ismej.2017.119.

Callahan, B. J., McMurdie, P. J., Rosen, M. J., Han, A. W., Johnson, A. J. A., and Holmes, S. P. (2016). DADA2: High-resolution sample inference from Illumina amplicon data. *Nature Methods* 13, 581–583. doi:10.1038/nmeth.3869.

Castañeda, L. E., Miura, T., Sánchez, R., and Barbosa, O. (2018). Effects of agricultural management on phyllosphere fungal diversity in vineyards and the association with adjacent native forests. *PeerJ* 6, e5715. doi:10.7717/peerj.5715.

Chao, A., Chazdon, R. L., Colwell, R. K., and Shen, T.-J. (2006). Abundance-based similarity indices and their estimation when there are unseen species in samples. *Biometrics* 62, 361–371. doi:10.1111/j.1541-0420.2005.00489.x.

Chen, H. (2018). *VennDiagram: Generate High-Resolution Venn and Euler Plots*. Available at: https://CRAN.R-project.org/package=VennDiagram.

Chiquet, J., Mariadassou, M., and Robin, S. (2018). Variational inference for sparse network reconstruction from count data. *arXiv:1806.03120 [stat]*. Available at: http://arxiv.org/abs/1806.03120 [Accessed June 20, 2018].

Cordier, T., Lanzén, A., Apothéloz-Perret-Gentil, L., Stoeck, T., and Pawlowski, J. (2018). Embracing environmental genomics and machine learning for routine biomonitoring. *Trends in Microbiology*. doi:10.1016/j.tim.2018.10.012.

Cougoul, A. P., Bailly, X., and Wit, E. C. (2019). MAGMA: inference of sparse microbial association networks. *bioRxiv*. doi:10.1101/538579.

Creamer, R. E., Hannula, S. E., Leeuwen, J. P. V., Stone, D., Rutgers, M., Schmelz, R. M., et al. (2016). Ecological network analysis reveals the inter-connection between soil biodiversity and ecosystem function as affected by land use across Europe. *Applied Soil Ecology* 97, 112–124. doi:10.1016/j.apsoil.2015.08.006.

Csardi, G., and Nepusz, T. (2006). The igraph software package for complex network research. *InterJournal* Complex Systems, 1695.

Das, P., Ji, B., Kovatcheva-Datchary, P., Bäckhed, F., and Nielsen, J. (2018). In vitro co-cultures of human gut bacterial species as predicted from co-occurrence network analysis. *PLOS ONE* 13, e0195161. doi:10.1371/journal.,pone.0195161.

Delière, L., Petitgenet, M., Goutouly, J.-P., Forget, D., Coulon, T., Davidou, L., et al. (2014). Le réseau Ecoviti Bordeaux expérimente des systèmes de culture viticoles « bas-intrants ». *Phytoma* 673, 51–55.

Delmas, E., Besson, M., Brice, M.-H., Burkle, L. A., Riva, G. V. D., Fortin, M.-J., et al. (2019). Analysing ecological networks of species interactions. *Biological Reviews* 94, 16–36. doi:10.1111/brv.12433.

Derocles, S. A. P., Bohan, D. A., Dumbrell, A. J., Kitson, J. J. N., Massol, F., Pauvert, C., et al. (2018). "Chapter One - Biomonitoring for the 21st Century: Integrating Next-Generation Sequencing Into Ecological Network Analysis," in *Advances in Ecological Research* Next Generation Biomonitoring: Part 1., eds. D. A. Bohan, A. J. Dumbrell, G. Woodward, and M. Jackson (Academic Press), 1–62. doi:10.1016/bs.aecr.2017.12.001.

Durán, P., Thiergart, T., Garrido-Oter, R., Agler, M., Kemen, E., Schulze-Lefert, P., et al. (2018). Microbial interkingdom interactions in roots promote *Arabidopsis* survival. *Cell* 175, 973-983.e14. doi:10.1016/j.cell.2018.10.020.

Edgar, R. C., and Flyvbjerg, H. (2015). Error filtering, pair assembly and error correction for next-generation sequencing reads. *Bioinformatics* 31, 3476–3482. doi:10.1093/bioinformatics/btv401.

European Commision (2007). Council Regulation (EC) No 834/2007 of 28 June 2007 on organic production and labelling of organic products and repealing Regulation (EEC) No 2092/91. *Official Journal of the European Union*, 1–23.

European Commision (2009). Directive 2009/128/EC of the European Parliament and of the Council of 21 October 2009 establishing a framework for Community action to achieve the sustainable use of pesticides. *Official Journal of the European Union*, 71–86.

Evans, D. M., Kitson, J. J. N., Lunt, D. H., Straw, N. A., and Pocock, M. J. O. (2016). Merging DNA metabarcoding and ecological network analysis to understand and build resilient terrestrial ecosystems. *Functional Ecology* 30, 1904–1916. doi:10.1111/1365-2435.12659.

Falkowski, P. G., Fenchel, T., and Delong, E. F. (2008). The microbial engines that drive Earth's biogeochemical cycles. *Science* 320, 1034–1039. doi:10.1126/science.1153213.

Faust, K., and Raes, J. (2012). Microbial interactions: from networks to models. *Nature Reviews Microbiology* 10, 538–550. doi:10.1038/nrmicro2832.

Freilich, M. A., Wieters, E., Broitman, B. R., Marquet, P. A., and Navarrete, S. A. (2018). Species co-occurrence networks: Can they reveal trophic and non-trophic interactions in ecological communities? *Ecology* 99, 690–699. doi:10.1002/ecy.2142.

Friedman, J., and Alm, E. J. (2012). Inferring correlation networks from genomic survey data. *PLoS Computational Biology* 8, e1002687.

Galan, M., Razzauti, M., Bard, E., Bernard, M., Brouat, C., Charbonnel, N., et al. (2016). 16S rRNA amplicon sequencing for epidemiological surveys of bacteria in wildlife. *mSystems* 1, e00032-16. doi:10.1128/mSystems.00032-16.

Gardes, M., and Bruns, T. D. (1993). ITS primers with enhanced specificity for basidiomycetes - application to the identification of mycorrhizae and rusts. *Molecular Ecology* 2, 113–118. doi:10.1111/j.1365-294X.1993.tb00005.x.

Gloor, G. B., Macklaim, J. M., Pawlowsky-Glahn, V., and Egozcue, J. J. (2017). Microbiome datasets are compositional: and this is not optional. *Front. Microbiol.* 8, 2224. doi:10.3389/fmicb.2017.02224.

Gramisci, B. R., Lutz, M. C., Lopes, C. A., and Sangorrín, M. P. (2018). Enhancing the efficacy of yeast biocontrol agents against postharvest pathogens through nutrient profiling and the use of other additives. *Biological Control* 121, 151–158. doi:10.1016/j.biocontrol.2018.03.001.

Hacquard, S., Spaepen, S., Garrido-Oter, R., and Schulze-Lefert, P. (2017). Interplay between innate immunity and the plant microbiota. *Annu. Rev. Phytopathol.* 55, 565–589. doi:10.1146/annurev-phyto-080516-035623.

Hassani, M. A., Durán, P., and Hacquard, S. (2018). Microbial interactions within the plant holobiont. *Microbiome* 6, 58. doi:10.1186/s40168-018-0445-0.

Ings, T. C., Montoya, J. M., Bascompte, J., Blüthgen, N., Brown, L., Dormann, C. F., et al. (2009). Review: Ecological networks – beyond food webs. *Journal of Animal Ecology* 78, 253–269. doi:10.1111/j.1365-2656.2008.01460.x.

Jaccard, P. (1900). Contribution au probleme de l'immigration post-glaciare de la flore alpine. *Bull Soc Vaudoise Sci Nat* 36, 87–130.

Jakuschkin, B., Fievet, V., Schwaller, L., Fort, T., Robin, C., and Vacher, C. (2016). Deciphering the pathobiome: intra- and interkingdom interactions involving the pathogen *Erysiphe alphitoides*. *Microbial Ecology* 72, 870–880. doi:10.1007/s00248-016-0777-x.

Kamada, N., Chen, G. Y., Inohara, N., and Núñez, G. (2013). Control of pathogens and pathobionts by the gut microbiota. *Nature Immunology* 14, 685–690. doi:10.1038/ni.2608.

Karimi, B., Maron, P. A., Boure, N. C.-P., Bernard, N., Gilbert, D., and Ranjard, L. (2017). Microbial diversity and ecological networks as indicators of environmental quality. *Environmental Chemistry Letters* 15, 265–281. doi:10.1007/s10311-017-0614-6.

Kemen, E. (2014). Microbe–microbe interactions determine oomycete and fungal host colonization. *Current Opinion in Plant Biology* 20, 75–81. doi:10.1016/j.pbi.2014.04.005.

Kemler, M., Witfeld, F., Begerow, D., and Yurkov, A. (2017). "Phylloplane Yeasts in Temperate Climates," in *Yeasts in Natural Ecosystems: Diversity*, eds. P. Buzzini, M.-A. Lachance, and A. Yurkov (Springer International Publishing), 171–197. doi:10.1007/978-3-319-62683-3_6.

Kernaghan, G., Mayerhofer, M., and Griffin, A. (2017). Fungal endophytes of wild and hybrid *Vitis* leaves and their potential for vineyard biocontrol. *Can. J. Microbiol.* 63, 583–595. doi:10.1139/cjm-2016-0740.

Koch, H., and Schmid-Hempel, P. (2011). Socially transmitted gut microbiota protect bumble bees against an intestinal parasite. *PNAS* 108, 19288–19292. doi:10.1073/pnas.1110474108.

Lafferty, K. D., Dobson, A. P., and Kuris, A. M. (2006). Parasites dominate food web links. *PNAS* 103, 11211–11216. doi:10.1073/pnas.0604755103.

Laur, J., Ramakrishnan, G. B., Labbé, C., Lefebvre, F., Spanu, P. D., and Bélanger, R. R. (2018). Effectors involved in fungal–fungal interaction lead to a rare phenomenon of hyperbiotrophy in the tritrophic system biocontrol agent–powdery mildew–plant. *New Phytol* 217, 713–725. doi:10.1111/nph.14851.

Layeghifard, M., Hwang, D. M., and Guttman, D. S. (2017). Disentangling Interactions in the microbiome: a network perspective. *Trends in Microbiology* 25, 217–228. doi:10.1016/j.tim.2016.11.008.

Love, M. I., Huber, W., and Anders, S. (2014). Moderated estimation of fold change and dispersion for RNA-seq data with DESeq2. *Genome Biology* 15, 550. doi:10.1186/s13059-014-0550-8.

Louca, S., Jacques, S. M. S., Pires, A. P. F., Leal, J. S., Srivastava, D. S., Parfrey, L. W., et al., (2016). High taxonomic variability despite stable functional structure across microbial communities. *Nature Ecology & Evolution* 1, 0015. doi:10.1038/s41559-016-0015.

Ma, A., Lu, X., Gray, C., Raybould, A., Tamaddoni-Nezhad, A., Woodward, G., et al. (2019). Ecological networks reveal resilience of agro-ecosystems to changes in farming management. *Nature Ecology & Evolution* 3, 260. doi:10.1038/s41559-018-0757-2.

Mace, G. M., Norris, K., and Fitter, A. H. (2012). Biodiversity and ecosystem services: a multilayered relationship. *Trends in Ecology & Evolution* 27, 19–26. doi:10.1016/j.tree.2011.08.006.

Macfadyen, S., Gibson, R., Polaszek, A., Morris, R. J., Craze, P. G., Planqué, R., et al. (2009). Do differences in food web structure between organic and conventional farms affect the ecosystem service of pest control? *Ecology Letters* 12, 229–238. doi:10.1111/j.1461-0248.2008.01279.x.

Makiola, A., Dickie, I. A., Holdaway, R. J., Wood, J. R., Orwin, K. H., Lee, C. K., et al. (2018). Biases in the metabarcoding of plant pathogens using rust fungi as a model system. *MicrobiologyOpen* 0, e780. doi:10.1002/mbo3.780.

McLaren, M. R., and Callahan, B. J. (2018). In nature, there is only diversity. *mBio* 9, e02149-17. doi:10.1128/mBio.02149-17.

McMurdie, P. J., and Holmes, S. (2013). phyloseq: An R package for reproducible interactive analysis and graphics of microbiome census data. *PLoS ONE* 8, e61217. doi:10.1371/journal.pone.0061217.

McMurdie, P. J., and Holmes, S. (2014). Waste not, want not: why rarefying microbiome data is inadmissible. *PLoS Computational Biology* 10, e1003531. doi:10.1371/journal.pcbi.1003531.

Morriën, E., Hannula, S. E., Snoek, L. B., Helmsing, N. R., Zweers, H., de Hollander, M., et al. (2017). Soil networks become more connected and take up more carbon as nature restoration progresses. *Nature Communications* 8, 14349. doi:10.1038/ncomms14349.

Montoya, D., Rogers, L., and Memmott, J. (2012). Emerging perspectives in the restoration of biodiversity-based ecosystem services. *Trends in Ecology & Evolution* 27, 666–672. doi:10.1016/j.tree.2012.07.004.

Murall, C. L., Abbate, J. L., Puelma Touzel, M., Allen-Vercoe, E., Alizon, S., Froissart, R., et al. (2017). "Invasions of Host-Associated Microbiome Networks," in *Advances in Ecological Research* (Elsevier), 201–281. doi:10.1016/bs.aecr.2016.11.002.

Oksanen, J., Blanchet, F. G., Friendly, M., Kindt, R., Legendre, P., McGlinn, D., et al. (2018). *vegan: Community Ecology Package*. Available at: https://CRAN.R-project.org/package=vegan.

Ovaskainen, O., Tikhonov, G., Norberg, A., Blanchet, F. G., Duan, L., Dunson, D., et al. (2017). How to make more out of community data? A conceptual framework and its implementation as models and software. *Ecology Letters* 20, 561–576. doi:10.1111/ele.12757.

Pancher, M., Ceol, M., Corneo, P. E., Longa, C. M. O., Yousaf, S., Pertot, I., et al. (2012). Fungal endophytic communities in grapevines (*Vitis vinifera* L.) respond to crop management. *Applied and Environmental Microbiology* 78, 4308–4317. doi:10.1128/AEM.07655-11.

Pauvert, C., Buée, M., Laval, V., Edel-Hermann, V., Fauchery, L., Gautier, A., et al., (2019). Bioinformatics matters: the accuracy of plant and soil fungal community data is highly dependent on the metabarcoding pipeline. *Fungal Ecology, online*. doi.org/10.1016/j.funeco.2019.03.005

Pecl, G. T., Araújo, M. B., Bell, J. D., Blanchard, J., Bonebrake, T. C., Chen, I.-C., et al. (2017). Biodiversity redistribution under climate change: Impacts on ecosystems and human well-being. *Science* 355, eaai9214. doi:10.1126/science.aai9214.

Pedersen, T. L. (2018). *ggraph: An Implementation of Grammar of Graphics for Graphs and Networks*. Available at: https://CRAN.R-project.org/package=ggraph.

Pellissier, L., Albouy, C., Bascompte, J., Farwig, N., Graham, C., Loreau, M., et al. (2018). Comparing species interaction networks along environmental gradients. *Biological Reviews* 93, 785–800. doi:10.1111/brv.12366.

Perazzolli, M., Moretto, M., Fontana, P., Ferrarini, A., Velasco, R., Moser, C., et al. (2012). Downy mildew resistance induced by *Trichoderma harzianum* T39 in susceptible grapevines partially mimics transcriptional changes of resistant genotypes. *BMC Genomics* 13, 660. doi:10.1186/1471-2164-13-660.

Pertot, I., Giovannini, O., Benanchi, M., Caffi, T., Rossi, V., and Mugnai, L. (2017). Combining biocontrol agents with different mechanisms of action in a strategy to control *Botrytis cinerea* on grapevine. *Crop Protection* 97, 85–93. doi:10.1016/j.cropro.2017.01.010.

Pielou, E. C. (1966). The measurement of diversity in different types of biological collections. *Journal of Theoretical Biology* 13, 131–144. doi:10.1016/0022-5193(66)90013-0.

Pilosof, S., Porter, M. A., Pascual, M., and Kéfi, S. (2017). The multilayer nature of ecological networks. *Nature Ecology & Evolution* 1, 0101. doi:10.1038/s41559-017-0101.

Pocock, M. J. O., Evans, D. M., and Memmott, J. (2012). The robustness and restoration of a network of ecological networks. *Science* 335, 973–977. doi:10.1126/science.1214915.

Poisot, T., Canard, E., Mouillot, D., Mouquet, N., and Gravel, D. (2012). The dissimilarity of species interaction networks. *Ecology Letters* 15, 1353–1361. doi:10.1111/ele.12002.

Poudel, R., Jumpponen, A., Schlatter, D. C., Paulitz, T. C., McSpadden Gardener, B. B., Kinkel, L. L., et al. (2016). Microbiome networks: a systems framework for identifying candidate microbial assemblages for disease management. *Phytopathology* 106, 1083–1096. doi:10.1094/PHYTO-02-16-0058-FI.

R Core Team (2017). *R: A Language and Environment for Statistical Computing*. Vienna, Austria: R Foundation for Statistical Computing Available at: https://www.R-project.org/.

Raimundo, R. L. G., Guimarães, P. R., and Evans, D. M. (2018). Adaptive Networks for Restoration Ecology. *Trends in Ecology & Evolution* 33, 664–675. doi:10.1016/j.tree.2018.06.002.

Ritpitakphong, U., Falquet, L., Vimoltust, A., Berger, A., Métraux, J.-P., and L'Haridon, F. (2016). The microbiome of the leaf surface of Arabidopsis protects against a fungal pathogen. *New Phytologist* 210, 1033–1043. doi:10.1111/nph.13808.

Röttjers, L., and Faust, K. (2018). From hairballs to hypotheses–biological insights from microbial networks. *FEMS Microbiol Rev* 42, 761–780. doi:10.1093/femsre/fuy030.

Sapkota, R., Knorr, K., Jørgensen, L. N., O'Hanlon, K. A., and Nicolaisen, M. (2015). Host genotype is an important determinant of the cereal phyllosphere mycobiome. *New Phytologist* 207, 1134–1144. doi:10.1111/nph.13418.

Scheffers, B. R., Meester, L. D., Bridge, T. C. L., Hoffmann, A. A., Pandolfi, J. M., Corlett, R. T., et al. (2016). The broad footprint of climate change from genes to biomes to people. *Science* 354, aaf7671. doi:10.1126/science.aaf7671.

Schieber, T. A., Carpi, L., Díaz-Guilera, A., Pardalos, P. M., Masoller, C., and Ravetti, M. G. (2017). Quantification of network structural dissimilarities. *Nature Communications* 8, ncomms13928. doi:10.1038/ncomms13928.

Schielzeth, H., and Nakagawa, S. (2013). Nested by design: model fitting and interpretation in a mixed model era. *Methods in Ecology and Evolution* 4, 14–24. doi:10.1111/j.2041-210x.2012.00251.x.

Schmid, F., Moser, G., Muller, H., and Berg, G. (2011). Functional and structural microbial diversity in organic and conventional viticulture: organic farming benefits natural biocontrol agents. *Applied and Environmental Microbiology* 77, 2188–2191. doi:10.1128/AEM.02187-10.

Schoch, C. L., Seifert, K. A., Huhndorf, S., Robert, V., Spouge, J. L., Levesque, C. A., et al. (2012). Nuclear ribosomal internal transcribed spacer (ITS) region as a universal DNA barcode marker for Fungi. *PNAS* 109, 6241–6246. doi:10.1073/pnas.1117018109.

Seufert, V., and Ramankutty, N. (2017). Many shades of gray—The context-dependent performance of organic agriculture. *Science Advances* 3, e1602638. doi:10.1126/sciadv.1602638.

Simpson, E. A. (1949). Measurement of species diversity. *Nature* 163, 688.

Simpson, G. L. (2016). *permute: Functions for Generating Restricted Permutations of Data*. Available at: https://CRAN.R-project.org/package=permute.

Swett, C. L., Bourret, T., and Gubler, W. D. (2016). Characterizing the brown spot pathosystem in late-harvest table grapes (*Vitis vinifera* L.) in the California Central Valley. *Plant Disease* 100, 2204–2210. doi:10.1094/PDIS-11-15-1343-RE.

Tackmann, J., Rodrigues, J. F. M., and Mering, C. von (2018). Rapid inference of direct interactions in large-scale ecological networks from heterogeneous microbial sequencing data. *bioRxiv*, 390195. doi:10.1101/390195.

Tilman, D., Cassman, K. G., Matson, P. A., Naylor, R., and Polasky, S. (2002). Agricultural sustainability and intensive production practices. *Nature* 418, 671–677. doi:10.1038/nature01014.

Tuck, S. L., Winqvist, C., Mota, F., Ahnström, J., Turnbull, L. A., and Bengtsson, J. (2014). Land-use intensity and the effects of organic farming on biodiversity: a hierarchical meta- analysis. *Journal of Applied Ecology* 51, 746–755. doi:10.1111/1365-2664.12219.

Tylianakis, J. M., Laliberté, E., Nielsen, A., and Bascompte, J. (2010). Conservation of species interaction networks. *Biological Conservation* 143, 2270–2279. doi:10.1016/j.biocon.2009.12.004.

Tylianakis, J. M., and Morris, R. J. (2017). Ecological networks across environmental gradients. *Annu. Rev. Ecol. Evol. Syst.* 48, 25–48. doi:10.1146/annurev-ecolsys-110316-022821.

Tylianakis, J. M., Tscharntke, T., and Lewis, O. T. (2007). Habitat modification alters the structure of tropical host–parasitoid food webs. *Nature* 445, 202–205. doi:10.1038/nature05429.

UNITE Community (2017). UNITE general FASTA release. doi:10.15156/BIO/587475.

Vacher, C., Tamaddoni-Nezhad, A., Kamenova, S., Peyrard, N., Moalic, Y., Sabbadin, R., et al. (2016). "Learning Ecological Networks from Next-Generation Sequencing Data," in *Advances in Ecological Research*, 1–39. doi:10.1016/bs.aecr.2015.10.004.

van der Heijden, M. G. A., Bardgett, R. D., and Straalen, N. M. V. (2008). The unseen majority: soil microbes as drivers of plant diversity and productivity in terrestrial ecosystems. *Ecology Letters* 11, 296–310. doi:10.1111/j.1461-0248.2007.01139.x.

Varanda, C. M. R., Oliveira, M., Materatski, P., Landum, M., Clara, M. I. E., and Félix, M. do R. (2016). Fungal endophytic communities associated to the phyllosphere of grapevine cultivars under different types of management. *Fungal Biology* 120, 1525–1536. doi:10.1016/j.funbio.2016.08.002.

Vayssier-Taussat, M., Albina, E., Citti, C., Cosson, J.-F., Jacques, M.-A., Lebrun, M.-H., et al. (2014). Shifting the paradigm from pathogens to pathobiome: new concepts in the light of meta-omics. *Frontiers in Cellular and Infection Microbiology* 4. doi:10.3389/fcimb.2014.00029.

Vogel, C., Bodenhausen, N., Gruissem, W., and Vorholt, J. A. (2016). The *Arabidopsis* leaf transcriptome reveals distinct but also overlapping responses to colonization by phyllosphere

commensals and pathogen infection with impact on plant health. *New Phytologist* 212, 192–207. doi:10.1111/nph.14036.

Wang, H., Wei, Z., Mei, L., Gu, J., Yin, S., Faust, K., et al., (2017). Combined use of network inference tools identifies ecologically meaningful bacterial associations in a paddy soil. *Soil Biology and Biochemistry* 105, 227–235. doi:10.1016/j.soilbio.2016.11.029.

Wang, Q., Garrity, G. M., Tiedje, J. M., and Cole, J. R. (2007). Naïve Bayesian classifier for rapid assignment of rRNA sequences into the new bacterial taxonomy. *Appl. Environ. Microbiol.* 73, 5261–5267. doi:10.1128/AEM.00062-07.

Watts, S. C., Ritchie, S. C., Inouye, M., and Holt, K. E. (2019). FastSpar: rapid and scalable correlation estimation for compositional data. *Bioinformatics* 35, 1064–1066. doi:10.1093/bioinformatics/bty734.

Weiss, S., Van Treuren, W., Lozupone, C., Faust, K., Friedman, J., Deng, Y., et al. (2016). Correlation detection strategies in microbial data sets vary widely in sensitivity and precision. *The ISME Journal* 10, 1669–1681. doi:10.1038/ismej.2015.235.

White, T. J., Bruns, T., Lee, S., and Taylor, J. (1990). Amplification and direct sequencing of fungal ribosomal RNA genes for phylogenetics. *PCR Protocols: A Guide to Methods and Applications*, 315–322.

Wickham, H. (2007). Reshaping data with the Reshape package. *Journal of Statistical Software* 21, 1–20.

Wickham, H. (2011). The split-apply-combine strategy for data analysis. *Journal of Statistical Software* 40, 1–29.

Wickham, H. (2016). *ggplot2: Elegant Graphics for Data Analysis*. Springer-Verlag New York Available at: http://ggplot2.org.

Wilke, C. O. (2018). *cowplot: Streamlined Plot Theme and Plot Annotations for "ggplot2."* Available at: https://CRAN.R-project.org/package=cowplot.

Zilber- Rosenberg, I., and Rosenberg, E. (2008). Role of microorganisms in the evolution of animals and plants: the hologenome theory of evolution. *FEMS Microbiology Reviews* 32, 723–735. doi:10.1111/j.1574-6976.2008.00123.x.

Zurell, D., Pollock, L. J., and Thuiller, W. (2018). Do joint species distribution models reliably detect interspecific interactions from co-occurrence data in homogenous environments? *Ecography* 41, 1812–1819. doi:10.1111/ecog.03315.

Zuur, A. F., Ieno, E. N., Walker, N., Saveliev, A. A., and Smith, G. M. (2009). *Mixed effects models and extensions in ecology with R*. New York, NY: Springer New York doi:10.1007/978-0-387-87458-6.

Supplementary Material

1. Supplementary Figures

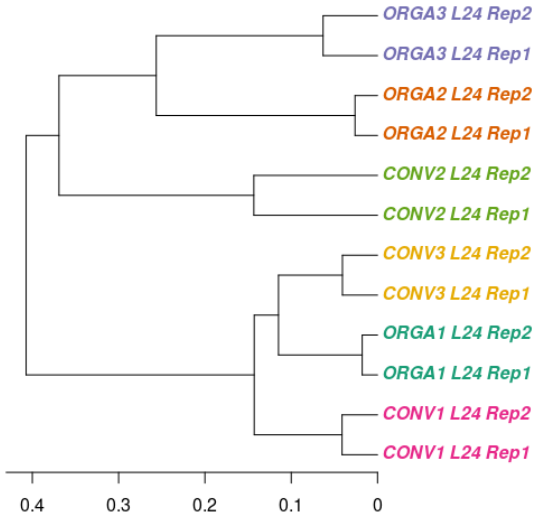

Figure S1 - Dendrogram plot of compositional dissimilarities between technical replicates for sequencing. Technical replicates were created by splitting six lots of PCR products in half and sequencing the two halves independently. The PCR products used were those corresponding to leaf 24 (L24) of the six plots studied (ORGA1, ORGA2, ORGA3, CONV1, CONV2, CONV3; see Figure 5). Compositional dissimilarities between samples were computed with the binary Jaccard index. The dendrogram was built using a hierarchical clustering algorithm (complete linkage method). Compositional dissimilarities between the two technical replicates of the same sample were significantly smaller than the dissimilarities among samples (PERMANOVA: $F = 39.98$; R2 = 0.97; $p = 0.001$).

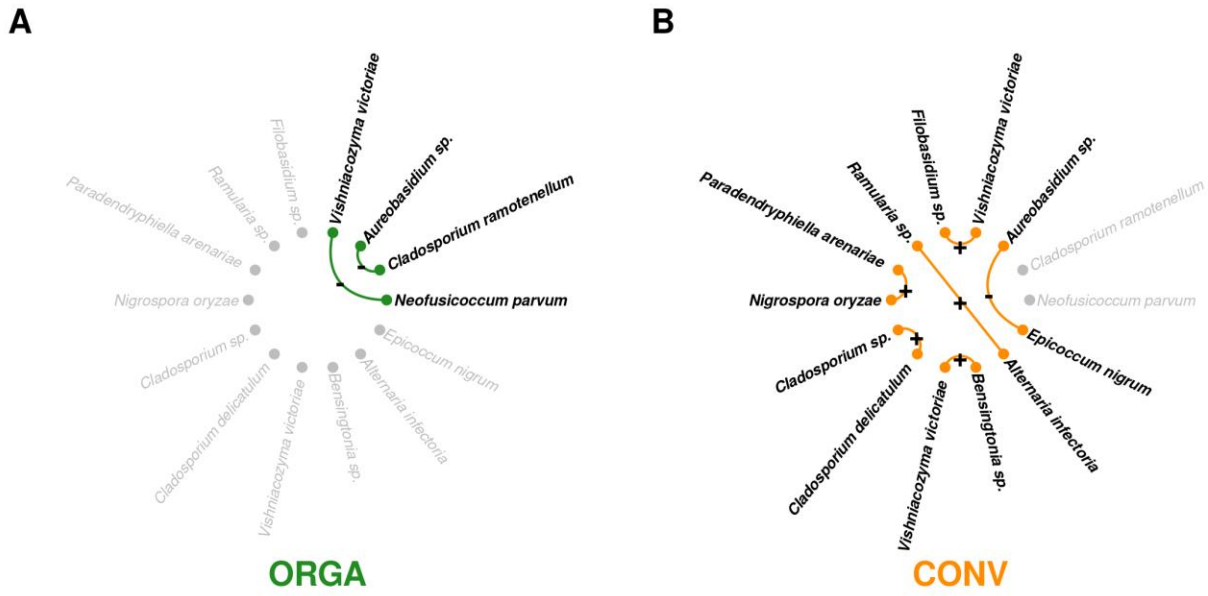

Figure S2 - Consensus fungal networks for (A) the organic (ORGA) and (B) the conventional (CONV) cropping systems. Network nodes represent fungal ASVs and links represent significant positive (+) or negative (-) associations shared bycommon to the three network replicates (Fig. 6A and 6B, respectively). The fungal ASVs absent from a network are indicated in gray.

2. Supplementary Tables

Table S1 - List of phytosanitary products and active ingredients applied in the year of the sampling campaign, together with the normalised dose or the treatment frequency index. PM = powdery mildew (caused by the fungal pathogen *Erysiphe necator*) and DM = downy mildew (caused by the oomycete pathogen *Plasmopara viticola*). Leaf sampling was performed on September 10 2015 (more than one month after the last phytosanitary treatment and a couple of hours before grape harvest). The treatment frequency index did not differ between cropping systems (ANOVA: df = 21; $F = 0.436$; $p = 0.516$).

Date	Cropping System	Fungicides	Active ingredients	Target disease	
				PM	DM
2015-04-30	ORGA	Heliocuivre©	Copper		0.145
2015-04-30	ORGA	Citrothiol DG©	Micronized sulfur	0.371	
2015-05-07	CONV	Chaoline©	Fosetyl aluminum + metirame		0.292
2015-05-07	CONV	Dynali©	Cyflufenamid + difenoconazole	0.289	
2015-05-13	ORGA	Heliocuivre©	Copper		0.167
2015-05-13	ORGA	Citrothiol DG©	Micronized sulfur	0.400	
2015-05-19	CONV	Cabrio Top©	Metirame-zinc + pyraclostrobin	0.500	
2015-05-28	ORGA	Citrothiol DG©	Micronized sulfur	0.800	
2015-05-28	ORGA	Bouillie Bordelaise RSR® Disperss® NC	Copper		0.533
2015-06-04	CONV	Vivando©	Metrafenone	0.833	
2015-06-04	CONV	Chaoline©	Fosetyl aluminum + metirame		0.708
2015-06-09	ORGA	Bouillie Bordelaise RSR® Disperss® NC	Copper		0.533
2015-06-09	ORGA	Citrothiol DG©	Micronized sulfur	0.600	
2015-06-25	ORGA	Citrothiol DG©	Micronized sulfur	0.600	
2015-06-25	CONV	Citrothiol DG©	Micronized sulfur	0.600	
2015-07-01	ORGA	Bouillie Bordelaise RSR® Disperss® NC	Copper		0.533
2015-07-01	CONV	Cabrio Top©	Metirame-zinc + pyraclostrobin	0.750	
2015-07-17	ORGA	Bouillie Bordelaise RSR® Disperss® NC	Copper		0.400

2015-07-17	ORGA	Heliocuivre©	Copper	0.083
2015-07-17	CONV	Bouillie Bordelaise RSR® Disperss® NC	Copper	0.400
2015-07-17	CONV	Heliocuivre©	Copper	0.083
2015-08-03	ORGA	Bouillie Bordelaise RSR® Disperss® NC	Copper	0.533
2015-08-03	CONV	Bouillie Bordelaise RSR® Disperss® NC	Copper	0.533

Table S2 - Effect of cropping system —conventional (CONV) *versus* organic (ORGA) — on the incidence and severity of foliar disease symptoms at harvest time (2015-09-07). Disease incidence is defined as the percentage of leaves displaying symptoms, whereas disease severity is defined as the percentage leaf damage. Symptom incidence and severity were estimated visually on 40 grapevines for each plot (40 × 3 per cropping system). The mean values are reported for each cropping system as a percentage. Wald χ^2 tests were used for comparisons after linear mixed model analysis with cropping system as a fixed effect and block as a random effect.

Disease		ORGA (%)	CONV (%)	χ^2	*p*-value
Downy Mildew	Incidence	0.749	0.688	0.57	0.450
	Severity	0.037	0.030	1.93	0.164
Powdery Mildew	Incidence	0.113	1.346	12.49	**<0.001**
	Severity	0.003	0.102	7.97	**0.005**
Black rot	Incidence	0.188	0.354	19.02	**<0.001**
	Severity	0.007	0.014	5.49	**0.019**

Table S3 - Primer pairs used to amplify the fungal ITS1 region

	1st PCR with regular primers (bold)
Forward	ITS1F: 5'-**CTTGGTCATTTAGAGGAAGTAA**-3'
Reverse	ITS2: 5'-**GCTGCGTTCTTCATCGATGC**-3'
	2nd nested PCR with pre-tagged primers (italics)
Forward	ITS1F-pre-tag: 5'- *CTTTCCCTACACGACGCTCTTCCGATCT***CTTGGTCATTTAGAGGAAGTAA**-3'
Reverse	ITS2-pre-tag: 5'-*GGAGTTCAGACGTGTGCTCTTCCGATCT***GCTGCGTTCTTCATCGATGC**-3'

Table S4 – Filtered ASV table. Samples are shown in columns, with amplicon sequence variants (ASV) in rows. The values indicated are sequence counts.

(Attached as csv file)

Table S5 - List of network α-properties calculated in this study

Network metric	Definition	Reference
Number of links (L)	Total number of links	
Connectance (C)	Fraction of the total number of possible links actually realized	Coleman and Moré 1983 10.1137/0720013
Number of connected components (CC)	Number of groups of nodes connected together	Martinez 1992 10.1086/285382
Diameter (DIA)	The longest of all the shortest paths between two nodes	Barabási et al., 2000 10.1016/S0378-4371(00)00018-2
Mean node degree (DEG)	Mean number of links per node	Martinez 1992 10.1086/285382
Proportion of negative links (NLR)	Proportion of links for which the SparCC correlation is negative	Faust et al., 2015 10.3389/fmicb.2015.01200

Table S6 - Effect of cropping system on the α-properties of fungal association networks. Properties (as defined in Table S3) were compared between cropping systems for every value of the percentage *P* of the most abundant ASVs used for network inference. The *U* and *p*-values of Wilcoxon rank-sum tests are reported. The *p*-value is not available (NA) for situations in which property values were equal for all networks. The *p*-values after Benjamini-Hochberg adjustment are not reported because all were equal to one.

P (%)	L	CC	DIA	C	DEG	NLR
10	$U = 3$; $p = 0.658$	$U = 5$; $p = 1$	$U = 6$; $p = 0.505$	$U = 3$; $p = 0.663$	$U = 2$; $p = 0.383$	$U = 5$; $p = 1$
20	$U = 1$; $p = 0.19$	$U = 6.5$; $p = 0.48$	$U = 8$; $p = 0.157$	$U = 2$; $p = 0.383$	$U = 1$; $p = 0.19$	$U = 9$; $p = 0.081$
30	$U = 1$; $p = 0.19$	$U = 4.5$; $p =$ NA	$U = 6$; $p = 0.619$	$U = 1$; $p = 0.19$	$U = 1$; $p = 0.19$	$U = 6$; $p = 0.663$
40	$U = 1$; $p = 0.19$	$U = 4.5$; $p =$ NA	$U = 7$; $p = 0.302$	$U = 2$; $p = 0.383$	$U = 1$; $p = 0.19$	$U = 5$; $p = 1$
50	$U = 3$; $p = 0.663$	$U = 4.5$; $p =$ NA	$U = 7$; $p = 0.302$	$U = 3$; $p = 0.663$	$U = 3$; $p = 0.663$	$U = 6$; $p = 0.663$
60	$U = 2$; $p = 0.383$	$U = 4.5$; $p =$ NA	$U = 4.5$; $p = 1$	$U = 2$; $p = 0.383$	$U = 1$; $p = 0.19$	$U = 5$; $p = 1$
70	$U = 3$; $p = 0.663$	$U = 4.5$; $p =$ NA	$U = 9$; $p = 0.047$	$U = 2$; $p = 0.383$	$U = 2$; $p = 0.383$	$U = 5$; $p = 1$
80	$U = 3$; $p = 0.663$	$U = 4.5$; $p =$ NA	$U = 6$; $p = 0.505$	$U = 4$; $p = 1$	$U = 3$; $p = 0.663$	$U = 4$; $p = 1$
90	$U = 4$; $p = 1$	$U = 4.5$; $p =$ NA	$U = 6$; $p = 0.505$	$U = 4$; $p = 1$	$U = 3$; $p = 0.663$	$U = 3$; $p = 0.663$
100	$U = 3$; $p = 0.663$	$U = 4.5$; $p =$ NA	$U = 4.5$; $p =$ NA	$U = 2$; $p = 0.383$	$U = 4$; $p = 1$	$U = 4$; $p = 1$

Table S7 - Effect of the percentage *P* of the most abundant ASVs used for network inference on the α-properties of fungal association networks. Spearman's correlation coefficient and the results of Spearman's rank correlation tests are reported for each network property. The *p*-values are reported after Benjamini-Hochberg adjustment.

Property	Correlation (ρ)	S	*p*-value
L	0.98	862	<0.001
CC	-0.61	57987	<0.001
DIA	-0.85	66635	<0.001
C	-0.67	60144	<0.001
DEG	0.95	1635	<0.001
NLR	-0.56	56116	<0.001